Mariner 6 and 7 Ultraviolet Spectrometer Experiment: Implications of CO_2^+, CO, and O Airglow

A. I. STEWART

Department of Astro-Geophysics and Laboratory for Atmospheric and Space Physics
University of Colorado, Boulder 80302

The Mariner 6 and 7 ultraviolet spectrometer experiments observed intense emissions from CO, O, and CO_2^+ in the Martian airglow. Analysis shows that they are excited predominantly by the absorption of solar EUV photons by CO_2 and constitute a major energy-loss mechanism for the thermosphere. Models of the thermospheric temperature profile and the airglow layer that demonstrate the effects of neutral chemistry and ionospheric composition are developed. With their aid, the observed CO Cameron-band emission scale height of 19 ± 4½ km is shown to suggest an exospheric temperature of 315 ± 75°K. Consideration of other data suggests a 'best' value of about 350°K. The emissions from CO_2^+ are consistent with a topside ionosphere containing about 30% CO_2^+. The abundance of O necessary to convert the rest to O_2^+ is about 2% at 135 km, in good accord with an independent determination. Within the uncertainties in the excitation efficiencies and in the thermospheric cooling mechanisms, the observations are consistent with the measured electron density. Eddy cooling may be important if the eddy diffusion coefficient is large, but it is difficult to reconcile the heating effects of CO_2 with the small observed airglow scale heights. There is no indication in the data that the ionosphere is modified by the solar wind below 200 km.

In recent years the Mariner series of planetary flyby missions has greatly stimulated discussion of the possible composition and thermal structure of the upper atmospheres of Mars and Venus. Radio occultation experiments carried on Mariners 4 and 5 measured electron-density profiles for the ionospheres of Mars [*Kliore et al.*, 1965*a*, *b*] and Venus [*Kliore et al.*, 1967], respectively, and an ultraviolet photometer on Mariner 5 observed Lyman-α radiation from the exosphere of Venus [*Barth et al.*, 1967]. The Mariner 5 results seemed consistent with a current theoretical view [*McElroy*, 1968] of the Venus upper atmosphere as consisting of essentially pure CO_2 with an exospheric temperature around 600°K and an ionosphere composed of CO_2^+ ions in local equilibrium between photoionization and dissociative recombination. The composition of the upper atmosphere of Mars was thought to be similar to that of Venus, but, to explain the Mariner 4 electron-density profile, it was necessary to postulate either that dynamical cooling affected the thermosphere on Mars to a much greater degree than on Venus [*Hogan and Stewart*, 1969] or that the Martian ionosphere was depressed by the solar wind [*McElroy*, 1969; *Cloutier et al.*, 1969]. A scarcity of atomic oxygen in the upper atmospheres of Mars and Venus, compared to the amount found on the earth, was suggested by the results of Mariner 4 [*Chamberlain and McElroy*, 1966], Mariner 5 [*Barth et al.*, 1967], and the Russian Venera 4 [*Kurt et al.*, 1968]. This scarcity was ascribed by *Shimizu* [1968, 1969] to a high degree of turbulence in the lower thermosphere and by *McElroy* [1967, 1968] to a rapid recombination of O and CO to form CO_2 via a chain of reactions involving CO_3*. In neither controversy did the data themselves offer any clue as to which, if either, of the postulates was correct.

The 1969 flyby missions to Mars by Mariner 6 and 7 offered the opportunity to examine its atmosphere in much greater detail than previously possible. The two spacecraft carried identical scanning ultraviolet spectrometer (UVS) experiments, one of the objectives being to detect and measure the airglow in the 1100- to 4300-A range. In this, as in their other objectives, the experiments were successful [*Barth et al.*, 1969]. The spectroscopic information, yielding the identities of major and minor con-

stituent gases in the upper atmosphere, and in some instances the nature of the excitation mechanisms as well, has been surveyed elsewhere [*Barth et al.*, 1971]. The intensity data [*Barth et al.*, 1971] yield the topside scale height of the emitting layer for the brighter features, and, for the brightest emission (the Cameron bands of CO), the peak and bottomside of the layer were observed as well. This latter fact permits the location of the observed layer on an atmospheric-pressure scale and greatly enhances the value of the UVS experiments as a tool for investigating thermospheric structure.

Another, more unexpected, feature of the UVS measurements renders them especially useful to this end. Although the emissions observed in the short-wavelength channel (1100–1900 A) are weak, their weakness indicating that those gases observed in resonance or fluorescent scattering in this channel (H, O, and CO) are minor constitutents only [*Anderson and Hord*, 1971; *Thomas*, 1971], the emissions in the long-wavelength channel (1900–4300 A) are very strong. In fact, more than 95% of the total airglow energy recorded by the instruments was received in the long-wavelength channel. The immediate inference is that these bright emissions arise as a direct result of the interaction of solar UV photons with the major constituent, CO_2. Thus the airglow-intensity profiles are very closely related to the distribution of CO_2 with altitude, that is, to the thermospheric-temperature profile. The UVS data can therefore be expected to yield reliable information about the temperatures in the Martian thermosphere.

In this paper, the origins of the bright airglow emissions are considered. A range of models of the temperature profile are developed, and airglow-intensity profiles are calculated from them. The models are developed with two ends in view. First, if a variety of physically reasonable models are available to compare to the data, it becomes a fairly simple matter to decide the range of temperatures in the thermosphere that is compatible with the UVS profiles and the excitation mechanisms that adequately reproduce the observed intensities. Second, the models demonstrate the influence on the calculated temperatures of the uncertainties in the mechanism that removes O from the thermosphere and in the composition of the ionosphere. Thus the implications of the UVS measurements regarding the airglow-excitation mechanisms, the thermospheric-temperature profile, and the processes controlling the thermospheric temperature and composition can be explored.

UVS Experiments and Results

The instruments, the data, and the data-reduction process have been described elsewhere [*Pearce et al.*, 1971; *Barth et al.*, 1969, 1971]. The following is a summary of those points that are particularly relevant to the present analysis.

The line of sight of the instruments scanned downward through the atmosphere above the bright limb of Mars 4 times, once at a point where the solar-zenith angle χ was 27°, once where it was 44° (the first 'limb crossings' of Mariner 6 and 7, respectively), and twice at the subsolar point where χ was 0° (the second limb crossings). A given spectral feature was scanned at altitude intervals of about 20 km, depending on the spacecraft velocity and the experimental geometry. The instrument's rectangular (2.3° × 0.23°) field of view was aligned nominally tangent to the planet's surface below the line of sight. The effective vertical extent of the field of view was about 40 km.

On each limb crossing, airglow emissions were clearly present in the long-wavelength channel (1900–4300 A) of five spectra, covering an altitude range of about 100 km. Figure 1 presents the measurements of the strongest of these emissions, which are to be discussed in detail. They are the $a^3\Pi$–$X^1\Sigma$ (Cameron) bands of CO, the ^3P–^1S (2972 A) multiplet of O, and the $\tilde{A}^2\Pi_u$–$\tilde{X}^2\Pi_g$ (Fox-Duffendack-Barker) and $\tilde{B}^2\Sigma_u^+$–$\tilde{X}^2\Pi_g$ ('doublet') bands of CO_2^+. The ^3P–^1S multiplet of O is accompanied by the much stronger ^1D–^1S branch at 5577 A, which is beyond the range of the UVS instrument.

The relative altitudes of the data points from a particular limb crossing are accurately known from the spacecraft trajectory data. Points from all four crossings were placed on a common altitude scale as follows. For each crossing, the point of maximum intensity of the CO Cameron bands was found by a simple curve-fitting procedure. This maximum was assumed to occur at the same altitude on all four crossings, thus removing the small effects of the variations of solar-zenith angle from the subsequent analysis,

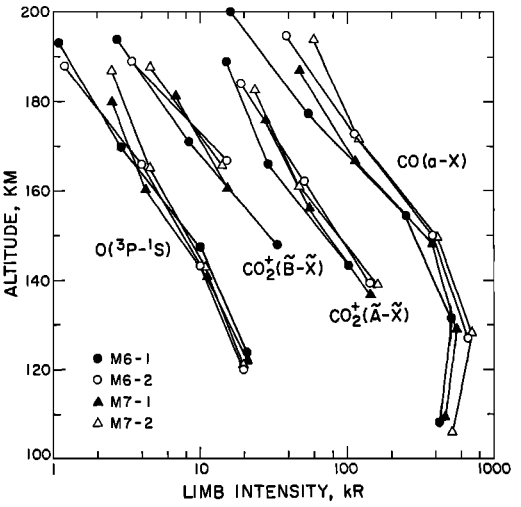

Fig. 1. Observed limb intensities of four airglow emissions. The different symbols distinguish the observations from each limb crossing. The closed circle represents Mariner 6, first limb crossing; open circle, Mariner 6, second limb crossing; closed triangle, Mariner 7, first limb crossing; open triangle, Mariner 7, second limb crossing.

which assumes a mean zenith angle of 20°. Since the shape of the emission profile of the Cameron bands is well defined in the data, the errors in this process are small, less than 5 km. The atmospheric models developed below were placed on an absolute altitude scale by requiring that, when χ equals 57°, the maximum electron density in the associated model ionospheres should occur at 135 km, which is in accordance with the results of radio occultation [*Fjeldbo et al.*, 1970]. The absolute altitude scale for the UVS data was then chosen to give the best over-all agreement between the data and the intensity profiles of the Cameron bands calculated for the models. Because of the similarity between the processes that produce the ionosphere and those that excite the Cameron bands, the error in this absolute scale is also small, not more than about 10 km. It arises largely from the uncertain altitude dependence near 135 km of quantities such as the ionospheric-recombination coefficient and the degree of scattered-light contamination of the measurements of the Cameron bands.

As seen in Figure 1, the observations from the four limb crossings agree very well with each other. There are, of course, differences in detail between one crossing and another, but the only suggestion of a systematic difference is that the measurements at the subsolar point (second crossings, open symbols) indicate slightly higher intensities and slightly larger topside scale heights than do the measurements at $\chi = 27°$ and 44° (first crossings, closed symbols). Any such differences will be ignored for the purposes of this paper.

The mean maximum limb intensity of the Cameron bands is 610 kR. The maximum of 21 kR for the O(^3P–^1S) multiplet implies that the associated (^1D–^1S) multiplet reaches 330 kR [*Garstang*, 1951]. The CO_2^+ band systems go off scale before reaching their maximum intensities; the greatest intensities recorded are 140 kR at 140 km for the $\tilde{A}$–$\tilde{X}$ system and 35 kR at 148 km for the $\tilde{B}$–$\tilde{X}$ system. The mean topside emission scale heights are obtained from the three highest data points on each limb crossing (two for the $CO_2^+(\tilde{B}$–$\tilde{X})$ bands) and thus refer to the approximate altitude range 150–190 km. The scale heights are 19 km for the CO Cameron bands, 24 km for the O multiplet, 24 km for the $CO_2^+(\tilde{A}$–$\tilde{X})$ bands, and 25 km for the $CO_2^+(\tilde{B}$–$\tilde{X})$ bands. The uncertainties in the intensities and scale heights will be discussed at appropriate points below. For comparison with the airglow data, the ionospheric scale height in the 150- to 190-km region is about 45 km [*Fjeldbo et al.*, 1970].

Although the observations in the 1100- to 1900-A region are not discussed here, use will be made of two results from the analysis by *Thomas* [1971], namely, that O and CO are scarce in the Martian thermosphere. The atomic-oxygen density was estimated from the observations of the resonance triplet near 1304 A, which is excited by the scattering of solar photons and by photoelectron impact on O and which is strongly affected by radiation trapping in the optically thick oxygen medium. Upper and lower limits on the CO density were set by considering, on the one hand, the amount of CO that would produce the observed intensity in the CO fourth positive bands by fluorescent scattering of sunlight alone, and, on the other hand, the amount of CO necessary to produce the observed amount of self-absorption in this same band system. The densities of O and CO at 135 km were found to be of the order of 3% and ½%, respectively.

IMPLICATIONS

Because of the geometry of the experiment and the relatively large sampling interval (20 km, comparable to the topside emission scale heights), no attempt is made to obtain volume emission rate from the limb-intensity data. The approach adopted is to construct models of the thermospheric-temperature profile and the airglow layer from which limb intensities may be calculated and compared directly to the measurements. This approach preserves the integrity of the data, and permits various experimental effects, such as the finite field of view, to be folded into the models rather than removed from the data. It also permits a straightforward evaluation by inspection of the agreement or lack of it between model and observation.

The comparison process divides itself into two steps, each yielding a different type of information. In the first step, the data are set against a range of models representing various alternatives as to heating and excitation processes. The comparison gives guidance about which excitation mechanisms or combination of mechanisms are adequate to produce the observed intensities and which temperature profile or range of profiles adequately reproduces the observed shape of the airglow layer. In the second step, the physical and chemical considerations that went into the building of the models and the estimated effects of those left out are discussed in the light of the conclusions drawn from the first step. The constraints placed by the UVS observations on processes and conditions in the actual Martian thermosphere at the time of the experiments can then be assessed. This section deals with the modeling of the thermosphere and airglow and performs the first step of the comparison; the second step is postponed to the discussion.

Excitation processes. The $\tilde{A}^2\Pi_u$–$\tilde{X}^2\Pi_g$ and $\tilde{B}^2\Sigma_u^+$–$\tilde{X}^2\Pi_g$ bands of CO_2^+ can be excited from neutral CO_2 by photoionization

$$CO_2 + h\nu \rightarrow CO_2^+ (\tilde{A}, \tilde{B}) + e \qquad (1)$$

or by impact of fast photoelectrons

$$CO_2 + e \rightarrow CO_2^+ (\tilde{A}, \tilde{B}) + 2e \qquad (2)$$

and from CO_2^+ ions by fluorescent scattering of sunlight

$$CO_2^+ (\tilde{X}) + h\nu \rightarrow CO_2^+ (\tilde{A}, \tilde{B}) \qquad (3)$$

The $\tilde{A}$ and $\tilde{B}$ states may also be populated by cascade from the $\tilde{C}^2\Sigma_g^+$ state. The experimental information on these processes was surveyed by *Dalgarno et al.* [1970], who found that the contribution of photoelectron impact, process 2, is not important on Mars. More recent experimental work [*Wauchop and Broida*, 1971; *Ajello*, 1971] confirms their conclusions. Although the bulk of the sun's ionizing radiation lies between 150 and 350 A [*Hinteregger*, 1970], no measurements of the branching ratios in photoionization, process 1, have been made at these wavelengths, and thus values based on the data at 584 A were used [*Turner and May*, 1967; *Spohr and von Puttkamer*, 1967; *Bahr et al.*, 1969; *Wauchop and Broida*, 1971], giving ratios for the $\tilde{X}$, $\tilde{A}$, $\tilde{B}$, and $\tilde{C}$ states of 0.33:0.33:0.22:0.11. The calculations presented below take account of the fact that part of the $\tilde{A}$–$\tilde{X}$ band system falls beyond the long-wavelength limit of the observations presented in Figure 1.

The observation of a limb intensity of around 600 kR in the Cameron bands at ionospheric altitudes (as evidenced by the simultaneous detection of emissions from CO_2^+) rules out excitation mechanisms involving ambient CO at the low densities deduced by *Thomas* [1971]. If the atmosphere at 135 km contains ½% CO, fluorescent scattering of sunlight produces a limb intensity of about 10 rayleighs at that altitude (the transition being optically forbidden), and photoelectron impact on CO produces not more than 25 kR, even though the cross section may be very large [*Hake and Phelps*, 1967; *Brongersma*, 1968]. It may be noted that a limb intensity of 600 kR implies a zenith intensity of about 30 kR, representing 30% of the energy in the incident solar ionizing flux [*Hinteregger*, 1970]. Similar remarks apply to the excitation of the ^3P–^1S multiplet of O. Three per cent atomic oxygen at 135 km yields not more than about 100 rayleighs by photoelectron impact, as compared to 21 kR observed; the $O(^1S)$ production implied by this observation represents 8% of the incident ionizing energy. Thus the important mechanisms for the production of $CO(a^3\Pi)$ and $O(^1S)$ must be those involving dissociative excitation of the major atmospheric constituent, CO_2, by solar photons

$$CO_2 + h\nu \rightarrow CO^* + O^* \qquad (4)$$

by fast photoelectrons

$$CO_2 + e \rightarrow CO^* + O^* + e \qquad (5)$$

or by photoionization and subsequent dissociative recombination

$$\left.\begin{aligned} CO_2 + h\nu &\rightarrow CO_2^+ + e \\ CO_2^+ + e &\rightarrow CO^* + O^* \end{aligned}\right\} \qquad (6)$$

The asterisks indicate that the products may be excited. A further possibility for the production of $O(^1S)$ is dissociative recombination of O_2^+

$$O_2^+ + e \rightarrow O + O^* \qquad (7)$$

for which the yield of $O(^1S)$ is 10% [*Feldman et al.*, 1971].

Because both $CO(a^3\Pi)$ and $O(^1S)$ are metastable, quantitative experimental investigation of processes 4–6 is more difficult than for processes 1–3, and much less information is available. *McConnell and McElroy* [1970] reviewed the position and estimated the relevant cross sections for photodissociation and photoelectron impact, processes 4 and 5. In performing the present calculations, it was considered desirable that the models should closely reproduce the Cameron-band intensities so that the temperature profile calculations should take proper account of this important energy loss. A secondary goal was to reproduce the $O(^3P\text{–}^1S)$ measurements. To these ends, the following otherwise arbitrary assumptions are made: Wherever energetically possible, the yield of $CO(a^3\Pi)$ and $O(^1S)$ in processes 4–6 is 100%, 75% being $CO(a^3\Pi)$ and 25% $O(^1S)$; wherever only $O(^1S)$ is accessible, its yield is 100%. In practice, the total excitation of the Cameron bands and the $O(^3P\text{–}^1S)$ multiplet by processes 4 and 5 together under these assumptions is very similar to that calculated by *McConnell and McElroy* [1970]; they make no estimate of the contribution from dissociative recombination, process 6.

The translation of the above information on excitation processes into predicted limb intensities for a given model atmosphere is relatively straightforward. The solar flux was taken from tabulations by *Hinteregger* [1970], *Hinteregger et al.* [1965], *Brinkmann et al.* [1966], and *Johnson* [1965], whereas the CO_2 absorption and photoionization cross sections came from *Inn et al.* [1953] and *Henry and McElroy* [1968]. Calculations of the effects of photoelectrons require knowledge of electron-impact excitation and ionization cross sections [*Hake and Phelps*, 1967; *Englander-Golden and Rapp*, 1964] and were performed according to the procedures described by *Dalgarno et al.* [1969]. Calculations of electron and ion densities involve the dissociative recombination coefficients for CO_2^+ and O_2^+, which have been measured by *Weller and Biondi* [1967] and *Kasner and Biondi* [1968]. The effects of minor constituents such as CO, O, and O_2 were not included. None of the emissions discussed here are subject to appreciable quenching in the thermosphere of Mars.

Model atmospheres and ionospheres. Details of the temperature profile calculations are given in the appendix. In this section, some aspects of particular relevance to the present analysis are discussed.

Atomic oxygen is known to be a product of photoabsorption by CO_2 at wavelengths below 2280 A, even at very low pressures [*Clark and Noxon*, 1970; *Felder et al.*, 1970]. The indications in the Mariner 4 and 5 data, mentioned in the introduction, that this oxygen is rapidly removed from the thermospheres of both Venus and Mars, are confirmed for Mars by the Mariner 6 and 7 UVS data near 1304 A [*Thomas*, 1971]. The two explanations offered for this removal differ greatly in their implications for thermospheric heating.

Shimizu [1968, 1969] proposed that the O and CO produced in the thermosphere is rapidly transported downward by strong turbulence to regions of higher pressure, where recombination proceeds via the three-body process

$$O + CO + M \rightarrow CO_2 + M \qquad (8)$$

If this is so, each pair of molecules, O and CO, carries with it 5.4 ev of chemical energy that is lost from the thermosphere, being ultimately released during the recombination reaction 8. From the work of *McElroy and Hunten* [1970] and of *Hunten and McElroy* [1970], it can be estimated that an eddy diffusion coefficient of about 3×10^7 cm^2 sec^{-1} is required to keep the O abundance at 135 km down to 3% of the ambient CO_2 density. The second explanation [*McElroy*, 1967, 1968] was that oxygen in the excited ^1D state, produced in the photodissociation of CO_2 at wavelengths less than 1670 A or in the recombination of the ionosphere, is removed in a chain of two-body reactions leading to the local recombination of CO_2

$$O(^1D) + CO_2 \rightarrow CO_3^* \quad (9)$$

$$CO_3^* + CO \rightarrow 2\ CO_2 \quad (10)$$

Here the chemical energy of the O and CO contributes directly to the thermospheric heating. Ground-state atomic oxygen, produced in photodissociation of CO_2 at wavelengths between 1670 and 2280 A and in reactions that quench $O(^1D)$, must still be removed by eddy transport, but a smaller eddy diffusion coefficient of about 5×10^8 cm^2 sec^{-1} seems adequate [*McElroy and Hunten*, 1970]. It is convenient to express the heating rate in terms of the 'heating efficiency' ϵ, which is the fraction of the total energy of the solar UV photons absorbed at a given altitude that appears locally as heat. The 5.4 ev per dissociation event, by which the heating in the two models differs, represents a change in ϵ of 0.29 in the upper thermosphere and of 0.55 in the lower thermosphere. (See Table 1.)

A third possibility arises if the CO_3^* produced in (9) reacts with O rather than with CO

$$CO_3^* + O \rightarrow CO_2 + O_2 \quad (11)$$

[See *McElroy and Hunten*, 1970.] Here the CO and O_2 carry away 2.9 ev per dissociation event; however, it is not necessary to invoke turbulence to explain the observed O density, since, at least in principle, reactions 9 and 11 can consume all the O produced in the thermosphere provided at least half is produced in singlet states. The density of atomic oxygen would then be controlled by photochemistry, and that of carbon monoxide controlled by diffusion.

The ionospheres calculated from the model atmospheres developed here are of the modified F_1-layer variety [*Donahue*, 1966]; the maximum electron density occurs at a pressure close to 8×10^{-4} μb when the solar zenith angle is 57° (the value appropriate to the occultation experiments). The composition of the ionosphere affects the heating efficiency, since the identity of the ion determines the amount of energy radiated by the excited products of dissociative recombination. Although CO_2^+ is the most abundantly produced ion, it is efficiently converted to O_2^+ by reactions with O

$$CO_2^+ + O \rightarrow O_2^+ + CO, \quad k = 1.6 \times 10^{-10}$$

$$CO_2^+ + O \rightarrow O^+ + CO_2, \quad k = 1.0 \times 10^{-10}$$

$$O^+ + CO_2 \rightarrow O_2^+ + CO, \quad k = 1.2 \times 10^{-9} \quad (12)$$

and also by reaction with O_2

$$CO_2^+ + O_2 \rightarrow O_2^+ + CO_2, \quad k = 5.0 \times 10^{-11} \quad (13)$$

where the reaction rates k are in cm^3 sec^{-1} [*Fehsenfeld et al.*, 1966*a*, 1966*b*; *Fehsenfeld et al.*, 1970]. Under the present assumption about the products of dissociative recombination, 5.1 ev is radiated per recombination in a CO_2^+ ionosphere, but only 0.2 ev is radiated in an O_2^+ ionosphere. The difference in the heating efficiencies in the two ionospheres is 0.11. (See Table 1.)

The effects of the minor constituents O and CO on thermospheric heating are not explicitly included in the calculations. Since CO^+ is rapidly converted to CO_2^+ by charge transfer [*Fehsenfeld et al.*, 1966*b*], the presence of CO has no effect on ionospheric composition, and excitation of the Cameron bands by photoelectron impact on CO at the observed densities causes a reduction in the heating efficiency by only 0.01; thus CO may reasonably be ignored. The most important effects of the presence of O are indirect. One

TABLE 1. Partition of Energy

Model	Kinetic Energy	Chemical Energy	Radiated in IR	Radiated in Airglow	Radiated in Cameron Bands
A (CO_2^+)	0.19 (0.33)	0.37 (0.66)	0.11 (0)	0.32 (0)	0.24 (0)
B (CO_2^+)	0.48 (0.88)	0.08 (0.12)	0.11 (0)	0.32 (0)	0.24 (0)
C (CO_2^+)	0.36 (0.64)	0.20 (0.35)	0.11 (0)	0.32 (0)	0.24 (0)
A (O_2^+)	0.30 (0.33)	0.37 (0.66)	0.11 (0)	0.21 (0)	0.14 (0)
B (O_2^+)	0.59 (0.88)	0.08 (0.12)	0.11 (0)	0.21 (0)	0.14 (0)
C (O_2^+)	0.46 (0.64)	0.20 (0.35)	0.11 (0)	0.21 (0)	0.14 (0)

effect, the conversion of CO_2^+ to O_2^+, has already been mentioned. The other important effect is that the energy of slow photoelectrons, which would otherwise go into vibrational excitation of CO_2 and be radiated in the infrared, may go into the excitation of the ^1D level of O and be converted by quenching into heat. Both effects can increase the heating efficiency by up to 0.11 if sufficient O is present. For a neutral atmosphere containing 3% O at 135 km and an ionosphere containing 30% CO_2^+ (as discussed below), the increase in ϵ over the pure CO_2, pure CO_2^+ situation is rather less than 0.11; the heating efficiencies in the CO_2^+ and O_2^+ models can be regarded as bracketing the values appropriate to the actual observations.

Temperature profiles calculated for various combinations of the oxygen-removal mechanisms and the ionospheric composition are presented in Figure 2. The label *A* denotes removal by strong turbulence and three-body recombination, reaction 8; *B* denotes removal by formation of CO_3^*, which subsequently reacts with CO, reactions 9 and 10; and *C* denotes the variation on *B* in which the CO_3^* reacts with O, reaction 11. The ionospheric composition is indicated in parentheses. The strong influence of the chemistry on the temperature is apparent; in the models *B*, the exospheric temperature T_∞ is about 130°K greater than in the models *A*. The conversion of all the CO_2^+ ions into O_2^+ increases T_∞ by between 35° and 55°K, largely because of the decreased radiation in the Cameron bands. The importance of the airglow emissions as an energy loss may be judged from the fact that if, in model $A(CO_2^+)$, the energy radiated in the Cameron bands is instead converted to heat, the exospheric temperature is raised from 333° to 432°K. The heating efficiencies and the temperatures at selected altitudes are tabulated for each model in the appendix.

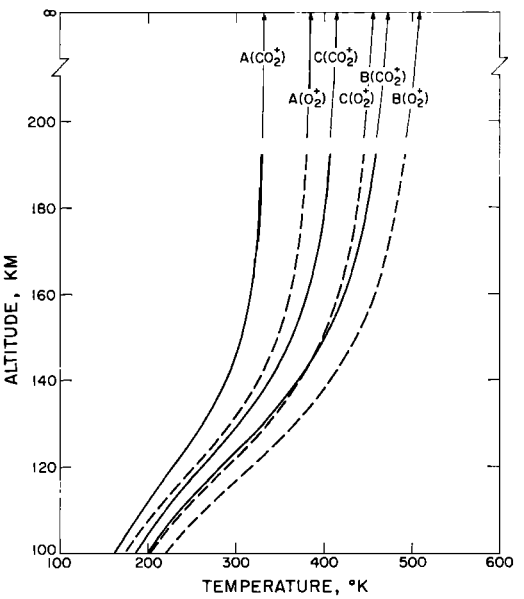

Fig. 2. Temperature profiles for six models of neutral and ionic recombination. Model A, neutral recombination proceeds via the reaction $O + CO + M \rightarrow CO_2 + M$; model B, via $CO_3 + CO \rightarrow CO_2 + CO_2$; model C, via $CO_3 + O \rightarrow CO_3 + O_2$. The composition of the ionosphere is indicated in parentheses. The altitude scale is discussed in the text.

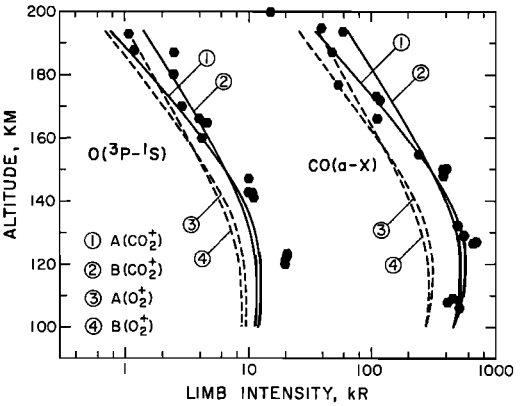

Fig. 3. Comparison between model airglow layers and observations for the Cameron bands of CO and the 2972-A emission of O. Hexagons are data points. Solid and dashed lines are used to represent the models for reasons of clarity.

Comparison with observation. The limb intensities calculated from the models are displayed in Figures 3 and 4, together with the data points. Figure 3 shows the CO Cameron band and the O^3P–^1S multiplet intensities, and Figure 4 shows the $CO_2^+\tilde{A}$–$\tilde{X}$ and $\tilde{B}$–$\tilde{X}$ band intensities. Curves for models $C(CO_2^+)$ and $C(O_2^+)$ are omitted for clarity; they fall approximately midway between those for models *A* and *B*. Because the CO_2^+ ion is a possible source of all the emissions, the model intensities depend on the ionospheric composition. They do not, however, depend on the neutral chemistry except indirectly through the temperature profiles. Two quantities will be used in the comparison of the models with the

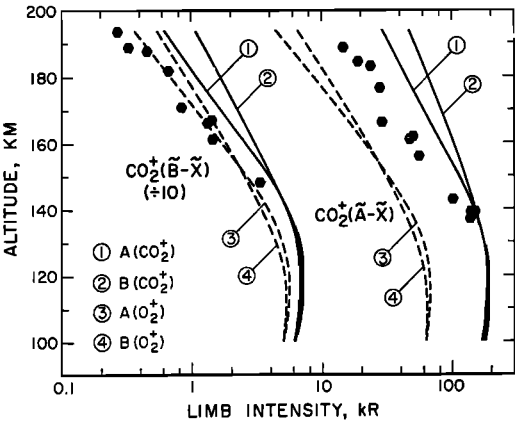

Fig. 4. Comparison between model airglow layers and observations for the $\tilde{A}$–$\tilde{X}$ and $\tilde{B}$–$\tilde{X}$ bands of CO_2^+. Hexagons are data points. Solid and dashed lines are used to represent the models for reasons of clarity.

data. The first, the emission scale height in the topside (150–190 km), reflects the temperature profile throughout the region where the optical depth for the ionizing solar radiations is less than unity ($Z \gtrsim 135$ km). The exospheric temperature is a reasonable parameter for this part of the profile. The second quantity, the maximum limb intensity, is determined by the solar EUV flux and the efficiency of the excitation mechanism acting on CO_2; for the CO_2^+ bands, the density of this ion also enters.

The determination of the topside scale height is affected by the removal from the raw data of off-axis scattered light, noise, and instrument background [*Barth et al.*, 1971]. Except at the lowest altitudes, the Cameron bands are almost entirely free of off-axis light, which arises from the scattering of sunlight from the lower atmosphere and surface of Mars and is therefore much weaker at short wavelengths than at long ones. Their scale height is therefore the most accurately determined. The group of data points near 194 km have a mean intensity of 36 kR, after subtracting corrections of about 45 kR each for instrument background and cosmic-ray noise. To the uncertainties of 3 and 9 kR, respectively, in these corrections, a statistical uncertainty of 4 kR must be added; a conservative estimate of the total uncertainty is thus 16 kR, the arithmetic sum of these components. This value, together with a less important uncertainty in the mean intensity of 350 kR for the points near 151 km, gives a topside scale height of 19 ± 4½ km. The corresponding quantities in models $A(CO_2^+)$, $A(O_2^+)$, $B(CO_2^+)$, and $B(O_2^+)$, which have exospheric temperatures of 333°, 386°, 474°, and 510°K, are 20, 23, 28, and 31 km. The Cameron-band measurements therefore indicate an exospheric temperature of 315 ± 75°K. This conclusion is in accord with a more subjective appraisal of Figure 3, which suggests that model $B(CO_2^+)$ offers a much poorer fit to the data than does model $A(CO_2^+)$. Model $B(CO_2^+)$ lies above all the data points near 194 and 172 km, but below all but one of the points near 151 km and below all of those near 129 km, whereas model $A(CO_2^+)$ passes through all the groups of points.

Since the excitation mechanisms are similar, the topside scale height of the $O(^3P\text{–}^1S)$ multiplet (24 km) must be interpreted in the same way as that of the Cameron bands. In effect, this is also true of the $CO_2^+(\tilde{B}\text{–}\tilde{X})$ system scale height (25 km) after a correction is made for the small contribution from fluorescent scattering; the correction is 3 km if the observed ionosphere contains 30% CO_2^+ (see below). Because of the greater degree of contamination by off-axis light, these values, 24 and 22 km, are less well-determined than the Cameron-band value of 19 km. A reasonable compromise is 21 km, corresponding to an atmosphere with an exospheric temperature of about 350°K. This value is then the 'best' one obtainable from the data. Little additional information regarding temperatures is contained in the $CO_2^+(\tilde{A}\text{–}\tilde{X})$ system observations because of the greater uncertainties. However, if the exospheric temperature is 350°K and if the ionosphere contains 35% CO_2^+, the present calculations reproduce the observed ratio of 2.8:1 between the intensities of the $\tilde{A}$–$\tilde{X}$ and $\tilde{B}$–$\tilde{X}$ systems at 160 km and predict a 31-km scale height for the $\tilde{A}$–$\tilde{X}$ system, in accord with the data within the errors.

Turning to the maximum limb intensities, the 610 kR in the Cameron bands and the 21 kR in the $O(^3P\text{–}^1S)$ multiplet, together with the implied 330 kR in the associated $O(^1D\text{–}^1S)$ multiplet, show that $CO(a^3\Pi)$ and $O(^1S)$ are produced in the ratio 63:37. *McConnell and McElroy* [1970] find 70:30 for the sum of processes 4 and 5, and the present analysis assumes 75:25. This ratio is in accord with the

data within the uncertainty in the relative calibration [*Pearce et al.*, 1971]. The agreement would be still better if the dissociative recombination of O_2^+ yields substantially more $O(^1S)$ than has been assumed here, as might occur if the O_2^+ produced by the reactions 12 is in high vibrational levels.

The models with a CO_2^+ ionosphere accurately reproduce the maximum Cameron-band intensity, since the excitation efficiencies were chosen with this reproduction in mind. However, the sum of the maximum observed slant column excitation rates of CO ($a^3\Pi$) and $O(^1S)$ is 9.6×10^{11} cm^{-2} sec^{-1}, whereas the CO_2^+ models predict only 7.5×10^{11} cm^{-2} sec^{-1} and the O_2^+ models 4.6×10^{11} cm^{-2} sec^{-1}. A deficiency in the solar EUV flux used is indicated by factors of 1.3 and 2.1, respectively, although the calibration uncertainty (a factor of 1.7) permits the data to be reconciled with the flux as used if the ionosphere contains 25% or more CO_2^+. The deficiency is naturally greater if the sum of the quantum yields of $CO(a^3\Pi)$ and $O(^1S)$ in processes 4–6 is less than the value of unity assumed here. With regard to the CO_2^+ band system intensities, photoionization alone fails to explain the data at 160 km by a factor of 1.8 ± 0.4. The discrepancy is removed if the ionosphere contains between 10 and 30% CO_2^+, but a larger EUV flux can be accommodated if photoionization between 150 and 350 A produces fewer excited ions than the measurements at 584 A suggest.

To summarize, the UVS measurements of Martian airglow emissions in the range 1900–4300 A suggest that the exospheric temperature lies in the range 315 ± 75°K, with a best value of about 350°K. The measurements are in accord with existing knowledge of the solar EUV flux and of the excitation mechanisms for these emissions if the Martian ionosphere contains about 30% CO_2^+. However, the data are also consistent with a solar EUV flux substantially greater than that measured by *Hinteregger* [1970]; an increase of a factor of 2 is readily reconciled with the data, and a greater increase cannot be ruled out.

DISCUSSION

Apart from the UVS results, only the radio occultation measurements of the electron-density profile provide any experimental information on the temperatures in the thermosphere of Mars. *Fjeldbo et al.* [1970] present their results in the form of a temperature of about 450°K, but the significance of this figure depends on the nature and composition of the ionosphere. If the topside of the observed ionosphere is in diffusive equilibrium, their temperature is the mean of the ion and electron temperatures and provides an upper limit to the neutral temperature. However, since the experimentally determined quantity is the plasma scale height, the deduced temperature depends on the mean ion mass. Fjeldbo et al. assumed that the ion was CO_2^+; if the ionosphere contains about 70% O_2^+, their temperature must be reduced to about 370°K, in good accord with the UVS results. It is much more likely that the ionosphere is in photochemical rather than diffusive equilibrium. [See, for example, *Johnson*, 1968.] In this instance the relationship between the plasma scale height and the neutral temperature is uncertain, being affected by altitude-dependent factors such as optical depth, ion and neutral composition, and recombination rates. In simple models the plasma scale height is roughly twice the neutral scale height, and thus there is no immediately apparent conflict between the measured plasma and airglow scale heights of about 45 and about 21 km, respectively, in the 150- to 190-km region.

Some theoretical temperature calculations appropriate to the Mariner 6 and 7 flybys have been published. *Stewart and Hogan* [1969] predicted exospheric temperatures of about 490°K, greater than all but one of the present models even though their EUV heating efficiency was quite small (0.35). Presumably, the reason is that they employed an augmented version of the solar ionizing flux measured by *Hinteregger et al.* [1965], which is more intense than the one used here [*Hinteregger*, 1970]. *McConnell and McElroy* [1970] present a model atmosphere with an exospheric temperature of 430°K and calculate a limb-intensity profile for the Cameron bands exhibiting a scale height of 26 km between 150 and 190 km. This figure is outside the limits set by the present analysis, and, in fact, the fit to the data provided by their model shows most of the shortcomings of the fit provided by model $B(CO_2^+)$ discussed earlier.

The UVS results provide the only experimental evidence on the composition of the Martian ionosphere. An internal consistency check is possible because of the conversion of CO_2^+ to O_2^+ by reactions 12 with O. In the absence of NO [*Barth et al.*, 1969], O_2^+ is the terminal ion, and dissociative recombination is the only loss process. Thus, in equilibrium,

$$kn(O)n(CO_2^+) = \alpha n_e n(O_2^+) \qquad (14)$$

where k is the effective rate constant of the reactions 12, α is the O_2^+ dissociative recombination coefficient, and the n's are the number densities of the indicated species. A knowledge of the electron density and ion composition at any altitude determines the density of O at that altitude, and a straightforward extrapolation yields the abundance of O at 135 km. Thus 30% CO_2^+ and 70% O_2^+ at 160 km, where $n_e = 1.1 \times 10^5$ cm^{-3} [*Fjeldbo et al.*, 1970], is consistent with 2% O at 135 km; less CO_2^+ implies more O. This result is in good accord with the entirely independent figure of about 3% obtained from analysis of the observations near 1304 A [*Thomas*, 1971].

Consideration of the maximum intensities in the previous section showed that the UVS measurements permitted a substantial increase in the adopted solar EUV flux, by a factor of up to about 2, with still larger increases being possible within the uncertainties in the excitation efficiencies. Further evidence for a greater flux comes from a comparison of the measured maximum electron density, 1.6×10^5 cm^{-3}, with the values of 7.6×10^4 cm^{-3} and 1.0×10^5 cm^{-3} calculated for CO_2^+ and O_2^+ ionospheres, respectively. An increase by a factor between 2.6 and 4.4 is indicated. However, increasing the ionizing flux by a factor of 2.5 raises the exospheric temperature in models $A(CO_2^+)$ and $A(O_2^+)$ by about 110°K, and an adjustment to the heating at longer wavelengths, or to the cooling, must be sought to restore the agreement between models and data.

Prag and Morse [1970] find that the solar vacuum UV flux is variable, and *Hall and Hinteregger* [1970] suggests that the 1325- to 1775-A flux used here may be too large by a factor of 3. A suitably reduced flux, however, lowers the exospheric temperature by only about 50°K. Cooling by infrared radiation from O and CO [see, for example, *McElroy et al.*, 1965] is a small effect and is more than balanced by the additional heating resulting from the conversion of CO_2^+ to O_2^+ by O. A potentially important cooling mechanism that is not included in the present models is eddy cooling, as suggested by *Johnson* [1966]. If the mechanical heating that must accompany the turbulence is ignored, the volume cooling rate is

$$L_E = -(d/dz)\{c_p \rho K[(dT/dz) + \Gamma]\} \qquad (15)$$

in which c_p is the specific heat at constant pressure, ρ the mass density, K the eddy diffusion coefficient, and Γ the adiabatic lapse rate (about 5°/km). A comparison of (15) with the volume heating rate shows that eddy cooling is a small effect in models B and C, in which K is 5×10^6 cm^2 sec^{-1} or less, but may be important in the models A, in which $K \simeq 3 \times 10^7$ cm^2 sec^{-1}. These conclusions are reinforced by the fact that the criterion suggested by *McElroy* [1967] for the suppression of eddy cooling by radiative relaxation effects is satisfied in models B and C but not in the models A. In the absence of an adequate description of the thermal effects of turbulence, the importance of eddy cooling remains problematical, but it is an attractive possibility.

With regard to the controversies that arose from the analysis of Mariner 4 and 5 results, Mariner 6 and 7 data offer clear evidence on one but not the other. *McElroy* [1969] and *Cloutier et al.* [1969] invoked a depression of the Martian ionosphere by the solar wind to reconcile the Mariner 4 plasma scale height of 29 km with a theoretical temperature profile showing an exospheric temperature of 487°K. They suggested that, at the time of Mariner 4, the plasma and neutral scale heights were in fact equal. This equality was clearly not true at the time of Mariner 6 and 7, at least below 200 km, where the plasma scale height is about 45 km and the airglow scale height is about 21 km. Since it seems unlikely that the exospheric temperature at the time of Mariner 4 should be substantially larger than the preferred value of 350°K deduced from the present analysis for Mariner 6 and 7, it is unlikely that their explanation of the Mariner 4 result is the true one. The view of *Hogan and Stewart* [1969] that the plasma scale height was small because the thermosphere was cold is much more in accord with the present results.

The only aspect of the present analysis that has a bearing on the question of the role of CO_3* in the Martian atmosphere is the difficulty of reconciling the warm thermospheres predicted in those models that include CO_3* chemistry [*McElroy*, 1969; and the present work] with the small observed airglow scale heights. When the laboratory evidence that CO_3* plays no important role in the photolysis of CO_2 is considered [*Young et al.*, 1968; *Clark and Noxon*, 1970; *Felder et al.*, 1970; *Slanger and Black*, 1970; *Loewenstein*, 1970], it is difficult to resist the conclusion that the agent responsible for the scarcity of O and CO in the Martian thermosphere is dynamical rather than chemical.

Summary and Conclusions

The scanning ultraviolet spectrometer experiments carried to Mars in the summer of 1969 by Mariner 6 and 7 provided the first opportunity to examine the upper atmosphere of another planet in detail. The spectra showed a rich and very intense airglow in the range 1900–4300 A, containing emissions from O, CO, and CO_2^+. The range 1100–1900 A also contained emissions from O and CO, but the total intensity was more than 20 times smaller. The inference that the long-wavelength emissions arise predominantly from the major atmospheric constituent, CO_2, whereas the short-wavelength emissions arise from much less abundant minor constituents, is supported by a more detailed examination of the excitation mechanisms. The UV airglow constitutes an important energy-loss mechanism for the Martian thermosphere, the emission from CO alone representing 30% of the energy measured in the incident ionizing solar flux. Thus the airglow is intimately related both to the distribution of CO_2 and to the heating mechanisms that determine this distribution.

To aid in the airglow analysis, models of the thermosphere were constructed by solving the heat balance equation, allowing for heating by UV absorption and for cooling by thermal conduction and radiation in the 15-μ bands of CO_2. The scarcity of minor constituents permitted their direct thermal effects to be ignored without serious error. The calculation of the heating efficiencies took into account the details of neutral and ion chemistry and of the airglow-excitation mechanisms, thus ensuring the consistency of the calculated temperature profiles and airglow intensities. The models that included CO_2 chemistry exhibited higher temperatures than those which did not because of the release of kinetic energy in the reactions of CO_2 with CO or O. The models that allowed for the conversion of CO_2^+ to O_2^+ by reaction with O were also warmer because dissociative recombination of CO_2^+ was assumed to excite emission in the Cameron bands of CO.

The highest quality data are those on the Cameron bands of CO that exhibit a topside emission scale height of 19 $\pm$ 4½ km. Comparison with the models shows that this implies an exospheric temperature of 315 $\pm$ 75°K. Consideration of other data as well suggests a best value of about 350°K. The data on the CO_2^+ band systems suggest that the ionosphere at 160 km contains about 30% CO_2^+; the remainder is most probably O_2^+. This result is in good accord with the atomic-oxygen abundance (3% at 135 km) deduced elsewhere from the UVS observations at 1304 A. Although the adopted solar flux explains all the data satisfactorily within the scale height and calibration uncertainties, an increase in the ionizing flux by a factor of up to 2 is not ruled out. The increase suggested by comparison of the calculated and observed electron density can be accommodated if the yields of excited species in the airglow-excitation mechanisms are less than has been assumed.

Such increases in the solar flux produce unacceptable increases in the calculated temperatures, and additional cooling must be invoked to explain the observed airglow scale heights. Eddy transport of heat is a likely possibility if the effective eddy diffusion coefficient is sufficiently large. It seems difficult, however, to reconcile the effects of CO_2 chemistry with the observations. The Mariner 6 and 7 radio occultation and UVS measurements do not support the view that the Martian ionosphere is depressed by the solar wind, at least below 200 km.

Appendix: Temperature Profiles of the Martian Thermosphere

The considerations that determine the temperature profiles in planetary thermospheres were first expounded by *Bates* [1951, 1959].

Chamberlain [1962] and *McElroy et al.* [1965] examined the atmosphere of Mars. More recent work by *McElroy* [1967, 1969] and by *Hogan and Stewart* [1969] embodied the knowledge gained from the analysis of the Mariner 4 and 5 results. The models developed here draw on most of the above work for the fundamental physics but treat some aspects in greater detail. They do not take account of dynamical effects, being of the 'planetary average' type in which the sun is assumed to shine for half of each day at an average solar-zenith angle of 60°. The calculated temperature profiles are used at and near the subsolar point on the assumption that the temperature at a given altitude is not greatly dependent on local time or on areographic latitude. As discussed in the text, the calculations are for a pure CO_2 atmosphere, the effects of minor constituents being ignored except for the action of O in transforming the major ion from CO_2^+ to O_2^+.

The simplified steady-state heat balance equation in pressure-temperature coordinates is

$$\frac{\partial}{\partial p}\left(C\frac{p}{H}\frac{\partial T}{\partial p}\right)+\frac{H}{p}(Q-L)=0 \qquad \text{(A1)}$$

in which p is the pressure, T the temperature, C the thermal conductivity, H the scale height, and Q and L the volume heating and radiative cooling rates, respectively. The barometric equation

$$dp/dz=-(p/H) \qquad \text{(A2)}$$

transforms the solutions to altitude (z) coordinates. Equation A1 was solved by using a simple relaxation technique, starting with an isothermal first trial. The boundary conditions are

$$Q=L \qquad \text{(A3)}$$

(local equilibrium) at the lower boundary, where $p=3.162\times10^{-2}$ μb, and

$$\partial T/\partial p=-(H^2/C)(Q/p) \qquad \text{(A4)}$$

at the upper boundary, where $p=0$ but Q/p remains finite. (A4) is equivalent to the condition that the atmosphere should be isothermal at very high altitudes. The thermal conductivity C was taken to be $0.33\times10^{-4}\ (T/273)^{1.5}$ cal cm^{-1} $°K^{-1}$ sec^{-1}; the evaluation of L and Q are described below.

Cooling. Cooling was assumed to occur only by radiation in the 15-μ band of CO_2. The volume cooling rate was taken to be

$$L=h\nu\cdot n^2\cdot\eta\cdot\exp\{-h\nu/kT\}\cdot F(\chi) \qquad \text{(A5)}$$

where $h\nu$ is the energy of a 15-μ photon, n is the local number density of CO_2, k is Boltzmann's constant, and the vibrational relaxation parameter η is represented by [*Simpson et al.*, 1969]

$$\eta=8.3\times10^{-15}\cdot T\cdot\exp\{-40.6T^{-1/3}\}\ \text{cm}^3\ \text{sec}^{-1} \qquad \text{(A6)}$$

$F(\chi)$ is a correction for the effects of radiation blanketing; according to *McElroy* [1967], the expression

$$F(\chi)=1-(1+\chi)e^{-\chi} \qquad \text{(A7)}$$

where

$$\chi=2.7\times10^9/n^2\eta \quad \text{for} \quad p\ll50\ \mu\text{b} \qquad \text{(A8)}$$

[*Chamberlain and McElroy*, 1966] is a satisfactory approximation. Inclusion of this correction has a negligible (<1°K) effect on the temperature profiles in Figure 2, and the present calculations set $F(\chi)=1$.

Heating. Although heating in CO_2 atmospheres can occur by absorption of infrared solar radiation, this effect is negligible in the upper thermosphere and reaches only about 15% at the lower boundary of the present models (R. E. Dickinson, private communication 1970). Heating is therefore assumed to occur only as a result of the absorption of ultraviolet photons. It depends on the partition of the photon energy into its several ultimate forms, kinetic energy of atoms and molecules, chemical energy of dissociation products, and energy radiated in the infrared, visible, and ultraviolet airglow.

The visible and ultraviolet emissions that carry away substantial amounts of energy on Mars are the $\tilde{A}$–$\tilde{X}$ and $\tilde{B}$–$\tilde{X}$ bands of CO_2^+, the ^1D–^1S multiplet of O, which is associated with the ^3P–^1S multiplet, and the Cameron bands of CO. The excitation mechanisms are discussed in the text. Various infrared transitions in CO_2 that are excited by nonthermal processes can properly be described as infrared airglow and are also important. Solar photons that are energetically incapable of causing dissociation of

CO_2 into the highly excited products involved in the airglow emissions may dissociate the molecule in lower continuums, producing CO in the ground state and O in the ground or ^1D states. Slow photoelectrons may either do the same or cause vibrational excitation of CO_2 either directly by collisions or indirectly by heating the ambient electron gas. This vibrational energy is most probably lost by radiation in the infrared. Other sources of vibrational energy, such as ion and neutral chemical reactions and the photodissociation process itself [*Clerc and Barat*, 1966], are ignored. Three mechanisms of neutral recombination and two of ionospheric recombination are considered, as described in the text. In all instances, it is assumed that the electronic energy of $O(^1D)$ is ultimately converted to heat. Where consistent with other assumptions and with energy considerations, it is assumed in the models *B* (recombination via the reaction of CO_3^* with CO) that O is produced in the ^1D state, and in the models *C* (reaction of CO_3^* with O) that one-half of the O is produced in singlet states. In the models *A* (three-body recombination), the state in which O is produced is immaterial.

Table 1 shows the partition of the energy in the various models considered. The photons responsible for exciting most of the airglow and for forming the ionosphere are absorbed rather abruptly near the 10^{-3} μb level; this absorption is reflected in the differences between the partition figures given for the limit of vanishingly small pressures (i.e., at the top of the thermosphere) and those figures given for $p = 3.162 \times 10^{-3}$ μb (near the bottom of the thermosphere). The latter figures are in parentheses. The quantity in the second column (Kinetic Energy) is called the heating efficiency in the text; it refers to a mean taken over all absorbed wavelengths, and thus it is not strictly comparable to the heating efficiencies of *Henry and McElroy* [1968] and of *Stewart and Hogan* [1969], which refer to ionizing wavelengths only.

Table 2 displays the temperature calculated for each model at the top of the thermosphere (i.e., the exospheric temperature), at the ionization maximum (135 km), and at 100 km. The profiles themselves are presented in Figure 2.

TABLE 2. Thermospheric Temperatures

Model	100 km, °K	135 km, °K	∞, °K
A (CO_2^+)	163	278	333
B (CO_2^+)	201	353	474
C (CO_2^+)	185	323	415
A (O_2^+)	175	313	386
B (O_2^+)	219	390	510
C (O_2^+)	203	358	457

Acknowledgments. It has been a privilege to work with the entire Mariner Ultraviolet Spectrometer team. My special thanks are due to C. A. Barth and G. E. Thomas for many useful discussions. I thank R. E. Dickinson for discussions of the temperature profile calculations.

This work was supported by the National Aeronautics and Space Administration grant NGL 06-003-052. I am indebted to the United Kingdom Science Research Council for a fellowship held at University College, London, during 1970–1971.

* * *

The Editor thanks M. B. McElroy and another referee for their assistance in evaluating this paper.

REFERENCES

Ajello, J. M., Emission cross sections of CO_2 by electron impact in the interval 1260 A to 4500 A, 2, *J. Chem. Phys., 55,* 1369, 1971.

Anderson, D. E., and C. W. Hord, Mariner 6 and 7 ultraviolet spectrometer experiment: Analysis of hydrogen Lyman-alpha data, *J. Geophys. Res., 76,* 6666, 1971.

Bahr, J. L., A. J. Blake, J. H. Carver, and V. Kumar, Photoelectron spectra and partial ionization cross sections for carbon dioxide, *J. Quant. Spectrosc. Radiat. Transfer, 9,* 1359, 1969.

Barth, C. A., J. B. Pearce, K. K. Kelly, L. Wallace, and W. G. Fastie, Ultraviolet emissions observed near Venus from Mariner 5, *Science, 158,* 1675, 1967.

Barth, C. A., W. G. Fastie, C. W. Hord, J. B. Pearce, K. K. Kelly, A. I. Stewart, G. E. Thomas, G. P. Anderson, and O. F. Raper, Mariner 6: Ultraviolet spectrum of Mars upper atmosphere, *Science, 165,* 1004, 1969.

Barth, C. A., C. W. Hord, J. B. Pearce, K. K. Kelly, G. P. Anderson, and A. I. Stewart, Mariner 6 and 7 ultraviolet spectrometer experiment: Upper atmosphere data, *J. Geophys. Res., 76,* 2213, 1971.

Bates, D. R., The temperature of the upper atmosphere, *Proc. Phys. Soc. London, Sect. B., 64,* 805, 1951.

Bates, D. R., Some problems concerning the terrestrial atmosphere above about 100 km, *Proc. Roy. Soc. London, Ser. A., 253,* 459, 1959.

Brinkmann, R. T., A. E. S. Green, and C. A. Barth, A digitalized solar ultraviolet spectrum, *Tech. Rep. 32-951,* Jet Propul. Lab., Pasadena, Calif., 1966.

Brongersma, H. H., Interaction of molecules with

low energy (0–30 ev) electrons, Ph.D. thesis, Univ. of Leiden, Leiden, Netherlands, 1968.

Chamberlain, J. W., Upper atmospheres of the planets, *Astrophys. J., 136,* 582, 1962.

Chamberlain, J. W., and M. B. McElroy, Martian atmosphere: The Mariner occultation experiment, *Science, 152,* 21, 1966.

Clark, I. D., and J. F. Noxon, Photodissociation of CO_2 on Mars, *J. Geophys. Res., 75,* 7307, 1970.

Clerc, M., and F. Barat, Cinétique des produits de decomposition de CO_2 par photolyse-éclair das l'ultraviolet lointain, *J. Chimie. Phys., 63,* 1525, 1966.

Cloutier, P. A., M. B. McElroy, and F. C. Michel, Modification of the Martian ionosphere by the solar wind, *J. Geophys. Res., 74,* 6215, 1969.

Dalgarno, A., M. B. McElroy, and A. I. Stewart, Electron impact excitation of the dayglow, *J. Atmos. Sci., 26,* 753, 1969.

Dalgarno, A., T. C. Degges, and A. I. Stewart, Mariner 6: Origin of Mars ionized carbon dioxide ultarviolet spectrum, *Science, 167,* 1490, 1970.

Detwiler, C. R., D. L. Garrett, J. D. Purcell, and R. Tousey, The intensity distribution in the ultraviolet solar spectrum, *Ann. Geophys., 17,* 263, 1961.

Donahue, T. M., Upper atmosphere and ionosphere of Mars, *Science, 152,* 763, 1966.

Englander-Golden, P., and D. Rapp, Total cross sections for ionization of atoms and molecules by electron impact, *Rep. LMSC 6-74-64-12,* Lockheed Missiles and Space Co., Palo Alto, Calif., 1964.

Fehsenfeld, F. C., A. L. Schmeltekopf, and E. E. Ferguson, Thermal energy ion-neutral reaction rates, 3, The measured rate constant for the reaction $O^+(^4S) + CO_2(^1\Sigma) \rightarrow O_2^+(^2\Pi) + CO(^1\Sigma)$, *J. Chem. Phys., 44,* 3022, 1966*a*.

Fehsenfeld, F. C., A. L. Schmeltekopf, and E. E. Ferguson, Thermal energy ion-neutral reaction rates, 5, Measured rate constants for C^+ and CO^+ reactions with O_2 and CO_2, *J. Chem. Phys., 45,* 23, 1966*b*.

Fehsenfeld, F. C., D. B. Dunkin, and E. E. Ferguson, Rate constants for the reaction of CO_2^+ with O, O_2 and NO; N_2^+ with O and NO; and O_2^+ with NO, *Planet. Space Sci., 18,* 1267, 1970.

Felder, W., W. Morrow, and R. A. Young, Experimental evidence of the photochemical instability of a pure CO_2 planetary medium, *J. Geophys. Res., 75,* 7311, 1970.

Feldman, P. D., J. P. Doering, and E. C. Zipf, Excitation of $O(^1S)$ atoms in the day airglow, *J. Geophys. Res., 76,* 3087, 1971.

Fjeldbo, G., A. Kliore, and B. Seidel, The Mariner 1969 occultation measurements of the upper atmosphere of Mars, *Radio Sci., 5,* 381, 1970.

Garstang, R. H., Energy levels and transition probabilities in p^3 and p^4 configurations, *Mon. Notic. Roy. Astron. Soc., 111,* 115, 1951.

Hake, R. D., Jr., and A. V. Phelps, Momentum-transfer and inelastic collision cross sections for electrons in O_2, CO, and CO_2 *Phys. Rev., 158,* 70, 1967.

Hall, L. A., and H. E. Hinteregger, Variations of incident solar EUV during a solar rotation, paper presented at 13th meeting of Cospar, Leningrad, May 21–30, 1970.

Henry, R. J. W., and M. B. McElroy, Photoelectrons in planetary atmospheres, in *The Atmospheres of Venus and Mars,* edited by J. C. Brandt and M. B. McElroy, p. 251, Gordon and Breach, New York, 1968.

Hinteregger, H. E., The extreme ultraviolet solar spectrum and its variations during a solar cycle, *Ann. Geophys., 26,* 547, 1970.

Hinteregger, H. E., L. A. Hall, and G. Schmidtke, Solar XUV radiation and neutral particle distribution in July 1963 thermosphere, *Space Res., 5,* 1175, 1965.

Hogan, J. S., and R. W. Stewart, Exospheric temperatures on Mars and Venus, *J. Atmos. Sci., 26,* 332, 1969.

Hunten, D. M., and M. B. McElroy, Reply to W. B. DeMore, *J. Geophys. Res., 75,* 4900, 1970.

Inn, E. C. Y., K. Watanabe, and M. Zelikoff, Absorption coefficients of gases in the vacuum ultraviolet, part 3, CO_2, *J. Chem. Phys., 21,* 1648, 1953.

Johnson, F. S., *Satellite Environment Handbook,* p. 123, Stanford University Press, Palo Alto, Calif., 1965.

Johnson, F. S., The atmosphere of Mars, paper presented at 7th meeting of Cospar, Vienna, May 10–19, 1966.

Johnson, F. S., Mariner 4 and the atmosphere of Mars, in *The Atmospheres of Venus and Mars,* edited by J. C. Brandt and M. B. McElroy, p. 181, Gordon and Breach, New York, 1968.

Kaplan, L. D., J. Connes, and P. Connes, Carbon monoxide in the Martian atmosphere, *Astrophys. J., 157,* L187, 1969.

Kasner, W. H., and M. A. Biondi, Temperature dependence of the electron-O_3^+-ion recombination coefficient, *Phys. Rev., 174,* 139, 1968.

Kliore, A. J., D. L. Cain, G. S. Levy, V. R. Eshleman, G. Fjeldbo, and F. D. Drake, Occultation experiment: Results of the first direct measurement of Mars atmosphere and ionosphere, *Science, 149,* 1243, 1965*a*.

Kliore, A. J., D. L. Cain, F. D. Drake, V. R. Eshleman, G. Fjeldbo, and G. S. Levy, Preliminary results of the Mariner 4 occultation measurements of the atmosphere of Mars, paper presented at Lunar and Planetary Conference, Calif. Inst. of Tech. Jet. Propul. Lab., Pasadena, Calif., Sept. 13–18, 1965*b*.

Kliore, A., G. S. Levy, D. L. Cain, G. Fjeldbo, and S. I. Rasool, Atmosphere and ionosphere of Venus from Mariner 5 *S*-band radio occultation measurement, *Science, 158,* 1683, 1967.

Kurt, V. G., S. B. Dostovalov, and E. K. Sheffer, The Venus far ultraviolet observations with Venera 4, *J. Atmos. Sci., 25,* 668, 1968.

Loewenstein, M., Relative quenching rates of

$O(^1D)$ by CO_2, N_2, and O_2 (abstract), *Eos Trans. AGU, 51,* 786, 1970.

McConnell, J. C., and M. B. McElroy, Excitation processes for Martian dayglow, *J. Geophys. Res., 76,* 7290, 1970.

McElroy, M. B., The upper atmosphere of Mars, *Astrophys. J., 150,* 1125, 1967.

McElroy, M. B., The upper atmosphere of Venus, *J. Geophys. Res., 73,* 1513, 1968.

McElroy, M. B., and D. M. Hunten, Photochemistry of CO_2 in the atmosphere of Mars, *J. Geophys. Res., 75,* 1188, 1970.

McElroy, M. B., J. l'Ecuyer, and J. W. Chamberlain, Structure of the Martian upper atmosphere, *Astrophys. J., 141,* 1523, 1965.

Pearce, J. B., K. A. Gause, E. F. Mackey, K. K. Kelly, W. G. Fastie, and C. A. Barth, The Mariner 6 and 7 ultraviolet spectrometer, *Appl. Opt., 10,* 805, 1971.

Prag, A. B., and F. A. Morse, Variations in the solar ultraviolet flux from July 13 to August 9, 1968, *J. Geophys. Res., 75,* 4613, 1970.

Shimizu, M., The recombination mechanism of O and CO in the upper atmospheres on Venus and Mars, *Icarus, 9,* 593, 1968.

Shimizu, M., A model calculation of the cytherean upper atmosphere, *Icarus, 10,* 11, 1969.

Simpson, C. J. S. M., T. R. D. Chandler, and A. C. Strawson, Vibrational relaxation in CO_2 and CO_2-Ar mixtures studied using a shock tube and a Laser-Schlieren technique, *J. Chem. Phys., 51,* 2215, 1969.

Slanger, T. G., and G. Black, The CO_2 photolysis problem (abstract), *Eos Trans. AGU, 51,* 786, 1970.

Spohr, R., and E. von Puttkamer, Energiemessung von Photoelektronen und Franck-Condon-Faktoren der Schwingungs Übergänge einiger Molikülionen, *Z. Naturforsch. A, 22,* 705, 1967.

Stewart, R. W., and J. S. Hogan, Solar cycle variation of exospheric temperatures on Mars and Venus: A prediction for Mariner 6 and 7, *Science, 165,* 386, 1969.

Thomas, G. E., Neutral composition of the upper atmosphere of Mars as determined from the Mariner UV spectrometer experiments, *J. Atmos. Sci., 28,* 859, 1971.

Turner, D. W., and D. P. May, Franck-Condon factors in ionization: Experimental measurement using molecular photoelectron spectroscopy, 2, *J. Chem. Phys., 46,* 1156, 1967.

Wauchop, T. S., and H. P. Broida, Cross sections for the production of fluorescence of CO_2^+ in the photoionization of CO_2 by 58.4 nanometer radiation, *J. Geophys. Res., 76, 21,* 1971.

Weller, C. S., and M. A. Biondi, Measurement of dissociative recombination of CO_2^+ ions with electrons, *Phys. Rev. Lett., 19,* 59, 1967.

Young, R. A., G. Black, and T. G. Slanger, Reaction and deactivation of $O(^1D)$, *J. Chem. Phys., 49,* 4758, 1968.

(Received January 18, 1971;
accepted September 21, 1971.)